Predistortion Technique for RF-Photonic Generation of High-Power Ultrawideband Arbitrary Waveforms

Bartosz Bortnik, Ilya Y. Poberezhskiy, *Member, IEEE*, Jason Chou, Bahram Jalali, *Fellow, IEEE, Fellow, OSA*, and Harold R. Fetterman, *Fellow, IEEE, Fellow, OSA*

***Abstract*—By employing an RF-photonic arbitrary waveform generator, the authors experimentally obtained complex high-power RF waveforms with spectra spanning more than a decade and voltage amplitudes of more than 13 V in a system limited by a gain ripple of up to 5 dB and phase distortion of over 200°. A spectral predistortion technique tailored to photonically assisted waveform generators that can overcome substantial RF amplifier gain ripple and phase distortion in order to generate high-power ($>$ 30 dBm) ultrawideband arbitrary RF waveforms is presented.**

***Index Terms*—Broadband amplifiers, microwave generation, optical fiber dispersion, optical signal processing, signal generators, spatial light modulators (SLMs).**

I. Introduction

COMPLEX high-power RF waveforms are useful in a variety of situations, including radar, ultrawideband (UWB) applications, and optical/electronic test and measurement. For instance, typical high-speed electrooptic devices (e.g., modulators, phase shifters, etc.) that can be driven at modulation frequencies reaching 50 GHz have a half-wave voltage of $\simeq 5$ V, and thus require high-speed RF waveforms with voltages of approximately 10 V to drive them through their entire range. Recently, optical approaches have been introduced to overcome limitations found in the electronic systems currently used to produce high-speed arbitrary signals [1]–[7]. Photonically assisted arbitrary waveform generators (AWGs) take advantage of the large bandwidth available in the optical domain, producing arbitrary RF waveforms with spectral content exceeding 60 GHz.

So far, the majority of these photonic AWG (PAWG) systems have been limited to the generation of low amplitude UWB signals on the order of 10 mV. Recently, a group at Purdue University realized UWB waveforms with voltage amplitudes of $\sim$ 400 mV in a direct space-to-time system utilizing a virtually imaged phased-array and a 20-GHz optical/electronic converter [1]. High-power amplification of wide bandwidth signals presents a significant challenge due to the severe amplitude and phase distortion in the gain spectrum of the state-of-the-art high-power broadband RF amplifiers.

Manuscript received August 1, 2005; revised March 31, 2006.

B. Bortnik, J. Chou, B. Jalali, and H. R. Fetterman are with the Electrical Engineering Department, University of California, Los Angeles, CA 90034 USA (e-mail: bartb@ucla.edu).

I. Y. Poberezhskiy was with the Electrical Engineering Department, University of California, Los Angeles, CA 90034 USA. He is now with the Jet Propulsion Laboratory, California Institute of Technology, Pasadena, CA 91109 USA.

Digital Object Identifier 10.1109/JLT.2006.875943

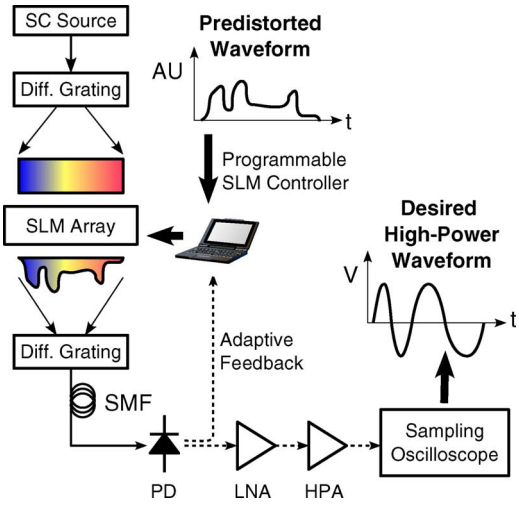

Fig. 1. RF photonic arbitrary waveform generator and amplifier cascade. A predistorted waveform is programmed into the PAWG and a desired high-power waveform is output. Solid and dashed lines denote optical and electrical connections, respectively. AU: arbitrary units, HPA: high-power amplifier, PD: photodetector, LNA: low-noise amplifier. (Color version available online at http://ieeexplore.ieee.org.)

In this paper, we propose and experimentally demonstrate a spectral predistortion technique that overcomes substantial gain spectrum fluctuations found in the RF portion of an RF-PAWG in order to generate high-power UWB microwave waveforms. Using the setup shown in Fig. 1, we produced an RF sawtooth waveform with a spectrum spanning more than a decade and voltage amplitudes of more than 13 V [7]. This waveform was obtained in a system impaired by a spectral gain ripple of up to 5 dB and phase distortion of over 200°. The waveform has a temporal aperture of 1.1 ns, and inexpensive system modifications produce continuous-wave (CW) waveforms. Our technique uses the experimentally obtained impulse response, along with considerations of the RF-PAWG, to calculate an inverse transfer function. Using this inverse transfer function, one can compute an appropriate predistorted input waveform for the RF-PAWG that will achieve a desired output waveform after high-power RF amplification.

It will be shown that simple spectral compensation does not suffice when using a PAWG capable of operating in a burst mode. This type of AWG is needed in applications requiring a waveform burst—a shaped waveform fragment spanning a finite time interval, e.g., in pulsed radar systems. It is illustrated below that due to the low-frequency attenuation of the high-power RF amplifier, simple spectral compensation requires a predistorted waveform that such a PAWG cannot generate. We

present a spectral-splicing technique that overcomes this difficulty and produces a predistorted waveform that is realizable by the PAWG and compensates for the system's distortions. Since our approach is software-based, it does not introduce any additional components into the PAWG system.

This paper is organized as follows. Section II gives a brief introduction to the RF-PAWG system and discusses the amplifiers used to amplify the UWB waveform. In Section III, we analytically describe our technique to overcome the challenges associated with photonic generation and subsequent amplification of a high-power UWB waveform. In Section IV, the implementation details are discussed, and the experimental results showing the generation of a high-power UWB waveform using our technique are presented. We conclude in Section V.

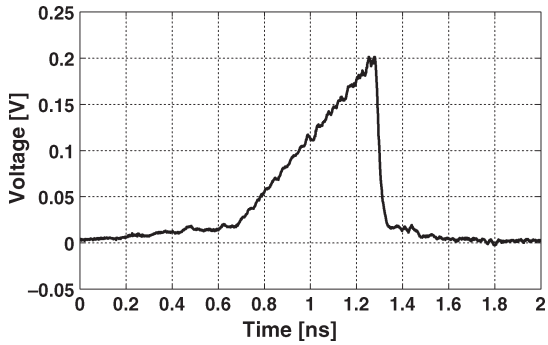

Fig. 2. High-speed 1.4-GHz sawtooth burst generated by the RF-PAWG system.

II. RF-PAWG System

A number of photonically assisted AWGs have been recently demonstrated. These systems include the virtually imaged phased-array system mentioned above [1]. In addition, a fiber-Bragg-grating sampling structure has produced continuous periodic 20-MHz sawtooth waveforms with an amplitude of approximately 17 V [2]. A system that adjusts the phase and magnitude of the individual longitudinal modes of a semiconductor mode-locked laser has achieved highly narrowband microwave tones [3]. Furthermore, Fourier synthesis of three CW semiconductor lasers has achieved continuous periodic trapezoidal waveforms of unspecified magnitude with a fundamental frequency of 9.4 GHz [4]. There was no mention of waveform amplification at the output of the system. Although these systems all vary in architecture, the predistortion technique presented in this paper is general enough so that it can be utilized to produce high-power waveforms in most amplified PAWG implementations.

Our PAWG system is based on a wavelength-to-time mapping and uses a programmable spatial light modulator (SLM) to shape the optical spectrum. The details of this adaptive RF-PAWG have been published elsewhere [5]. Here, we review its general operation and the challenges associated with generating a high-power RF waveform.

The basic concept of this PAWG is illustrated in Fig. 1. Supercontinuum (SC) generation in nonlinear optical fibers creates a broadband optical pulse. Bandwidths exceeding 200 nm are readily achieved using short lengths of conventional dispersion-shifted fiber [8]. The pulse spectrum is bandpass filtered to 20 nm and incident upon a high-resolution SLM. Individual pixels of the SLM apply precise levels of attenuation to sculpt an arbitrary waveform onto the spectrum. The light is then focused into a single-mode fiber (SMF-28). Dispersive effects in the SMF create a one-to-one mapping between wavelength and time, converting the spectral modulation into a time-domain amplitude modulation. The length of the dispersive fiber determines the temporal duration of the signal. Due to the wavelength-to-time mapping of the dispersive fiber, the temporal envelope of the optical waveform has an intensity variation that upon photodetection directly corresponds to the electrical signal. Using commercially available components, instantaneous frequencies exceeding 60 GHz can be achieved. The RF-PAWG generates finite-duration burst waveforms that repeat at a period determined by the broadband source laser. The operation of this system in a continuous mode is published elsewhere [9].

In this system, the programmable SLM offers a high degree of flexibility and efficiency in waveform generation, without the need for manufacturing a dedicated spatial mask or adjusting fiber-Bragg-grating locations and reflectivities. Furthermore, as indicated in Fig. 1, we are able to implement a software-based adaptive feedback algorithm that adjusts the voltage on the SLM pixels by comparing the temporal output waveform directly after the photodetector with the desired waveform. This algorithm compensates for system distortions, such as imperfect matching of the spectrum to the SLM pixels, beam shape, and optical spectrum fluctuations that would otherwise deform the temporal signal.

We have chosen to focus our attention on generating sawtooth waveforms due to their distinguishing characteristics. Most notably, these waveforms have a slow ramping portion and a sharp "flyback" region and thus require a wide bandwidth to be produced at high fidelity. Sawtooth waveforms can be used as the driving signal of an optical phase modulator in order to perform serrodyne frequency shifting [10]. The technique in this paper was successfully employed to generate an ultrafast sawtooth waveform at a sufficient power to produce an optical serrodyne frequency shift significantly exceeding the previously published results [11]. Here, we detail the encountered RF distortions, discuss the inherent limitations of the PAWG, and introduce a predistortion technique based on spectral splicing that overcomes these obstacles to generating high-speed high-power arbitrary waveforms. This paper will present implementation details, experimental results, and describe the limitations of this technique.

The sawtooth waveforms generated by our system had spectra that spanned 0–25 GHz, requiring high-bandwidth RF components. Fig. 2. shows a sawtooth waveform produced by our system. It has a 670-ps rise time and a 50-ps flyback time, corresponding to a fundamental frequency of $\simeq$ 1.4 GHz. Since this waveform has spectral content well into tens of gigahertz, it is currently not possible to produce this waveform using an electronic AWG.

The photonic waveform is detected in a broadband photodetector with a 3-dB bandwidth of 50 GHz. A typical unamplified

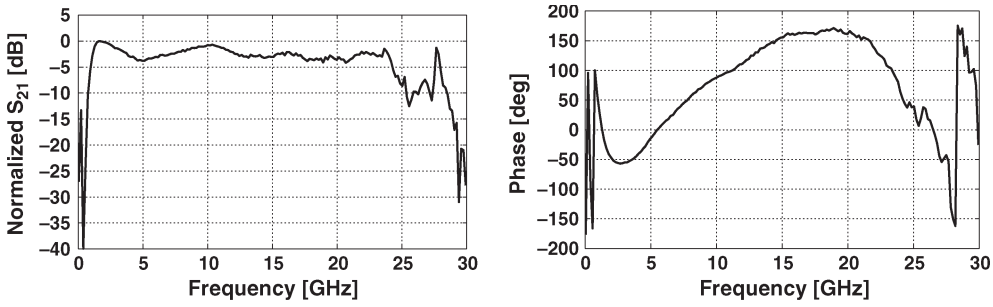

(a) (b)

Fig. 3. (a) Magnitude of the high-power amplifier's S_{21} scattering parameter. An amplitude ripple of ~ 4 dB is observed. (b) Phase of the high-power amplifier's S_{21} scattering parameter. A phase ripple of over 200° is observed.

high-speed photodetector operating in the 1.55-μm wavelength region has a response of about 1 A/W or 50 V/W into a 50-Ω load impedance matched to typical 50-Ω cables and connectors. Most high-speed photodetectors have a saturation threshold on the order of 0-dBm optical power and therefore are limited to yielding signals below 100 mV. To produce a high-power waveform with an amplitude of 10 V, we needed to increase the voltage amplitude by nearly three orders of magnitude, or almost six orders of magnitude in power, while preserving the temporal shape of the waveform. Obtaining such high gain required cascading solid-state UWB amplifiers in series (shown in Fig. 1). A low-noise UWB amplifier (Agilent 83050A) was used right after the photodetector. It was followed by a high-power solid-state amplifier (Agilent 83020A) capable of producing 1-W output over the 1–26.5-GHz range. Together, these amplifiers had a rated gain of over 50 dB.

High-power amplifiers are typically used for CW or narrowband signals. Little attention is paid to the fluctuations of gain, and particularly phase, across the spectrum, since only a small fraction of the bandwidth is used in practice at any given time. Furthermore, it is difficult to design a high-power high-bandwidth solid-state amplifier with a flat gain spectrum. Typically, multiple stages of integrated amplification are used in both series and parallel configurations. It becomes increasingly difficult to control spectral fluctuations with each additional stage. Whereas most lower power broadband amplifiers are designed to have a gain ripple of ± 3 dB or less, the Agilent 83020A has a specified gain ripple of ± 5 dB typical. The amplifier's phase distortion is unspecified.

Since our signal is UWB, it is highly vulnerable to the gain and phase fluctuations in the amplifier's spectrum. We measured the nonideal high-power amplifier's transfer function using a vector network analyzer to characterize its behavior. Fig. 3(a) and (b) shows the amplifier's S_{21} scattering parameter, both magnitude and phase response, as a function of frequency from 0.45 MHz to 30 GHz. The amplifier contains a substantial gain ripple of $\simeq 4$ dB across the frequency range of 2–24 GHz, and, due to the severe drop around 25 GHz, the gain ripple increases to more than 10 dB. Furthermore, the phase response varies by over 200° across the spectrum, making high-fidelity amplification of a desired UWB signal impossible. In addition, the nonideal frequency response of various components in the system, such as the photodetector, RF cables, connectors, and isolators, can add to distortion of the signal. The effect of the amplifier distortion is illustrated in Fig. 4, which shows the output of the amplifier when the sawtooth of Fig. 2 is used as the input.

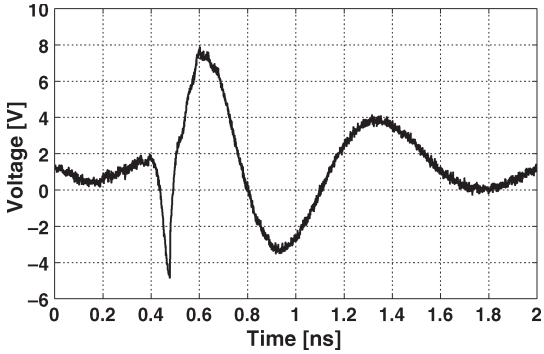

Fig. 4. Distorted output after RF amplification of the waveform in Fig. 2.

III. Predistortion Algorithm

We have developed a predistortion technique where the RF-PAWG generates a predistorted waveform that accounts for the distortions in the RF portion of the system, namely from the high-power amplifier. The flexible nature of our programmable RF-PAWG is well suited for this approach. This technique does not require the insertion of any compensating circuitry or filters into the system since it is entirely implemented in software. Below, we detail our algorithm, which compensates for both the RF limitations of the amplifier and waveform generation limitations of the PAWG. This technique is general enough so that the predistortion algorithm can be applied to other high-power PAWG systems.

The PAWG initially generates, at high fidelity, an optical signal with an intensity envelope corresponding to the desired waveform. In our system, this is performed by the SLM and dispersive fiber. Let $S_0(f)$ denote the Fourier transform of this high-fidelity optical intensity envelope. In most UWB PAWG systems, f will span from DC to tens of gigahertz.

Once the signal $S_0(f)$ is photodetected, it passes through multiple amplifiers, isolators, cables, and other RF components before arriving at its destination. Let us call $H(f)$ the transfer function of the totality of these components. Thus, we anticipate a distorted signal $D(f)$ at the output

$$D(f) = H(f)S_0(f). \tag{1}$$

Our goal is to develop a number of operations performed on $S_0(f)$ that produce a predistorted waveform denoted as $P(f)$. By inputting the predistorted waveform $P(f)$ into the system with transfer function $H(f)$ we hope to obtain a desired output waveform $S(f)$ that is similar to our ideal waveform $S_0(f)$. Let us denote each operation onto $S_0(f)$ as $\hat{G}_i$, and the application of all of these operators as $\hat{G} = \hat{G}_1\hat{G}_2, \ldots, \hat{G}_k$. Using the predistorted waveform as the input, we can rewrite (1) as

$$S(f) = H(f)\hat{G}S_0(f) = H(f)P(f). \tag{2}$$

It will be shown that three operations are used to produce an acceptable predistorted signal.

A. Spectral Inversion

The first operator $\hat{G}_1$ performs a spectral compensation of the system's transfer function by inverting $H(f)$. Since $H(f)$ is complex, this inversion compensates for both gain and phase fluctuations in the spectrum. However, only a portion of the spectrum can be inverted, since most high-frequency RF amplifiers have a finite passband. Below the lower cutoff frequency f_l and above the upper cutoff frequency f_h, the magnitude of the transfer function $H(f)$ is close to zero, and, hence, its inverse is very large. Attempting to apply the inverse of this transfer function onto $S_0(f)$ grossly emphasizes exceptionally low and high frequency components, washing out the important characteristics attained by inversion in the range of $f_\mathrm{l} \leq f \leq f_\mathrm{h}$. Thus, $H(f)$ should only be inverted within this range. We define the spectral-inversion operator as

$$\hat{G}_1 S_0(f) = \begin{cases} 0, & f < f_\mathrm{l} \\ (1/H(f))\, S_0(f), & f_\mathrm{l} \leq f \leq f_\mathrm{h} \\ 0, & f_\mathrm{h} < f \end{cases}. \tag{3}$$

In practice, setting the higher portion of the spectrum to zero for $f > f_\mathrm{h}$ has minor consequences. High frequency components are responsible for sharp transitions in the temporal curve. The loss of these components may smooth out these transitions, but the overall shape of the signal is preserved. In addition, many of the systems' RF components strongly attenuate high frequencies, and, thus, their compound effect prohibits the transmission of these high frequencies in the first place.

In contrast, setting the lower portion of the spectrum to zero for $f < f_\mathrm{l}$ has three important consequences. First, since $H(f)$ is complex, it contains important phase information. While the magnitude of $H(f)$ is smaller at frequencies slightly below f_l than within the range $f_\mathrm{l} \leq f \leq f_\mathrm{h}$, it may still contain important phase information—particularly right at the band edge. The spectral-inversion operator of (3) discards this phase information for $f < f_\mathrm{l}$ in the predistorted waveform.

Second, setting the lower part of the spectrum to zero creates a sharp discontinuity at $f = f_\mathrm{l}$. This also is true if we set $\hat{G}_1 = 1$ for $f < f_\mathrm{l}$. In either case, this sharp characteristic in the frequency domain corresponds to slow oscillations that occur over a long time scale in the predistorted waveform. Most burst mode AWGs, including our RF-PAWG, by definition, generate a waveform over a finite time interval in a single shot, or burst, fashion. Lengthy temporal characteristics cannot be properly generated, and hence, the AWG is incapable of generating a signal with sharp spectral features. This limitation of the PAWG introduces distortions into the predistorted waveform. Furthermore, due to its highpass nature, the high-power amplifier generates slow oscillations of its own. These oscillations limit the length of controllable temporal features in the signal, and by extension, the length of a desired high-fidelity waveform. Since oscillations with a period above $1/f_\mathrm{l}$ are filtered out by the amplifier, the desired high-fidelity waveform should have a length that is less than this period.

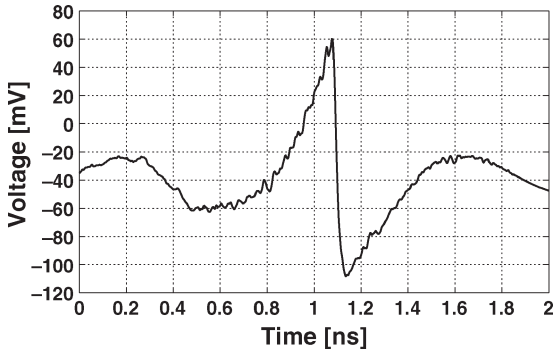

Fig. 5. Simulated output of the experimentally attained sawtooth of Fig. 2 passed through an ideal highpass filter with a 1-GHz cutoff.

Last and most importantly, setting the waveform spectrum to zero for $f < f_\mathrm{l}$ gives $\hat{G}_1$ a highpass filter behavior, lowering the entire temporal waveform. To examine this, let us consider the output of an ideal highpass filter when an experimentally obtained sawtooth fragment with a fundamental frequency of 1.4 GHz (Fig. 2) is the input. We have set the cutoff frequency to $f_\mathrm{l} = 1$ GHz. Fig. 5 shows the simulated temporal output of this highpass filter. This waveform is the best achievable in a perfect system where there are no spectral gain or phase fluctuations except for the highpass behavior of the high-power amplifier. Eliminating the low frequency components has the effect of swinging portions of the waveform below the zero-voltage level.

This highpass filtering behavior of the spectral-inversion operator is problematic because the waveform shown in Fig. 5 is impossible for the PAWG to generate. In a PAWG, the signal is shaped optically and ultimately converted to an electrical signal through photodetection. When no light is incident on the photodetector, the photodetector outputs a "dark voltage." It is not possible to generate an electrical signal with a voltage that is lower than the dark voltage. Even if a DC offset is added or subtracted from the signal, it will still be impossible to produce a voltage that is less than the dark voltage, adjusted for the DC offset. For this reason, we will call the dark-voltage level the voltage floor and explain the consequence of this limitation below.

B. PAWG Voltage-Floor Limitation

The voltage-floor limitation of the PAWG system is a significant obstacle in the pursuit of predistorting the waveform. As described above, the highpass nature of the spectral-inversion operator $\hat{G}_1$ produces a signal that swings below the zero-voltage level, or in a practical PAWG system, the voltage

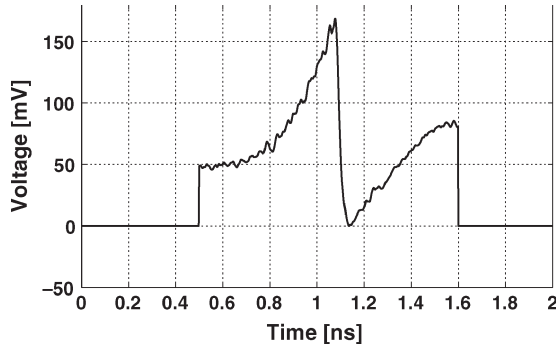

Fig. 6. Simulated raised and windowed version of Fig. 5 illustrating the PAWG's voltage-floor limitation and finite programmable time interval.

floor. Thus, unless the algorithm above is altered, the spectral-inversion operator produces a predistorted waveform that the PAWG cannot generate. To address this difficulty, we have developed a technique that generates a predistorted waveform that is entirely above the voltage floor. This technique also addresses the discontinuity of phase and amplitude at $f = f_{\rm l}$ that the spectral-inversion operator $\hat{G}_1$ will inevitably produce. We term our technique "spectral splicing" and present it in depth below. However, first, we will discuss a simpler technique that may come to mind when attempting to address the difficulty mentioned above—to simply raise and window the waveform. While this "raise and window" technique seems straightforward, it also possesses several significant disadvantages. We have incorporated a part of this technique into spectral splicing while mitigating its unwanted effects.

Perhaps, the most intuitive method of bringing the waveform above the voltage floor is to set the lowest point of the programmed temporal signal equal to the voltage floor. Recall that PAWGs operating in burst mode generate a waveform fragment that spans some maximum time interval τ, and then the signal drops to the voltage floor for a time $T - \tau$ until the next waveform burst. For instance, the waveform of Fig. 2 can only be shaped over a time interval of $\tau \simeq 1$ ns. To bring the waveform above the voltage floor, the waveform that is programmed into the PAWG is raised by the difference between the voltage floor and the minimum voltage of the waveform. However, the PAWG is able to manipulate the signal only during the interval of the waveform burst. Outside the burst's interval of τ, the signal remains at the voltage floor for a time $T - \tau$.

In this case, the PAWG would produce the simulated waveform depicted in Fig. 6. In essence, we have "raised and windowed" the waveform, i.e., raised and multiplied it by a $\mathrm{rect}(t/\tau)$ with a width of τ. This produces a sharp jump up from and back down to the voltage floor at the leading and trailing edges of the waveform, respectively. These sharp transitions indicate a significant change in the waveform's higher frequencies by the windowing and raising processes. Unfortunately, these jumps generate significant oscillations at the output of the RF amplifier and, thus, inhibit the amplification of a high-fidelity waveform. They are also responsible for sharp artifacts at the beginning and end of the output waveform. Moreover, these sharp transitions exacerbate any nonlinearities and resonances within the RF amplifier's circuitry, further distorting the signal.

C. Spectral Splicing

The spectral-inversion operator $\hat{G}_1$ performs an excellent job of predistortion within the range $f_{\rm l} \leq f \leq f_{\rm h}$, and it is in our interest to preserve its effect in this frequency range. When the components below $f < f_{\rm l}$ are attenuated, the time-domain signal swings below the voltage floor. It stands to reason that adding components to this portion of the spectrum, while retaining the inverted spectrum of $\hat{G}_1 S_0$ above $f_{\rm l}$, can produce a predistorted temporal signal that is above the voltage floor and has smooth transitions at the waveform's edges. We propose a spectral-splicing technique where the inverted spectrum for $f \geq f_{\rm l}$ is merged with the inverted spectrum that has been temporally raised and windowed. The operators $\hat{G}_2$ and $\hat{G}_3$ are introduced below to perform this spectral-splicing operation on the waveform. These operators insert frequency components that elevate the waveform. Furthermore, this technique does not produce the sharp transitions at the beginning and trailing edges of the temporal waveform, since we are only altering the low-frequency portion of the inverted spectrum. Moreover, the addition of the lower frequency components to the predistorted waveform's spectrum has no effect on the ultimate shape of the high-power waveform, since the amplifier does not pass the low frequency components.

While it is easier to calculate the spectral-splicing operation partially in the time domain, we will present this operation entirely in the frequency domain for consistency. A discussion on performing part of the calculation in the time domain is given in Section IV. Recall that the inversion operator $\hat{G}_1$ spectrally inverts the signal, while simultaneously swinging the temporal waveform below the voltage-floor level. Let $I(f) = \hat{G}_1 S_0(f)$ denote the spectrally inverted signal and its time-domain representation as $i(t)$. First, we must raise the temporal signal by the minimum value of the waveform $\min(i(t))$ by adding this value to its DC component $I(f = 0)$. We introduce the raising operator

$$\hat{G}_2 I(f) = \begin{cases} I(0) - \min\left(i(t)\right), & f = 0 \\ I(f), & f \neq 0 \end{cases}. \tag{4}$$

Let $R(f) = \hat{G}_2 I(f)$ denote the raised and spectrally inverted waveform. After raising the waveform, we apply a window spanning the duration of the desired waveform by multiplying with a $\mathrm{rect}(t/\tau)$ or convolving it in the frequency domain with a $\tau \mathrm{sinc}(\tau f)$. This windowed version is then spectrally spliced with the unwindowed version of the sawtooth. We introduce the spectral-splicing operator that performs this process:

$$\hat{G}_3 R(f) = \begin{cases} \tau \mathrm{sinc}(\tau f) \star R(f), & f < f_{\rm l} \\ R(f), & f \geq f_{\rm l} \end{cases} \tag{5}$$

where $\star$ denotes the convolution in the frequency domain.

D. Minimum PAWG Temporal Aperture

To be effective, the spectral-splicing operator must insert frequency components below $f_{\rm l}$ that produce temporal variations within the time scale of the predistorted waveform's duration. Since the predistorted waveform's duration is limited by the

PAWG's temporal aperture τ, this condition places a constraint on τ as a function of $f_{\rm l}$. To further examine this constraint, let us consider a simplified form of the spectral-splicing algorithm where a sinusoid with period 2τ is added to the spectrally inverted waveform. The sinusoid's phase is set such that an all-positive half cycle overlaps with the PAWG's output interval. The addition of this sinusoid acts to raise the center portion of the waveform without increasing the signal near the waveform's edges. In contrast, the addition of a sinusoid with a period that is significantly greater than 2τ will be unable to raise the waveform without simultaneously creating a sharp transition at either or both endpoints. Furthermore, the frequency of this additional sinusoid must also fall below $f_{\rm l}$ in order to preserve the ultimate shape of the output waveform after the high-power amplifier. Thus, we conclude that the predistorted waveform's duration τ cannot be smaller than $1/2f_{\rm l}$ when using a spectral splicing, otherwise, no meaningful frequencies can be inserted into the waveform's spectrum.

While this places a lower limit on the predistorted waveform's duration, and in turn the PAWG's temporal aperture, the minimum acceptable duration that yields a high-fidelity waveform will likely be larger. In practice, the PAWG's finite temporal aperture physically windows the predistorted waveform. This temporal windowing equates to convolution of the entire predistorted waveform's spectrum with a sinc, making analysis beyond the simple case above difficult. Nonetheless, we have found that $\tau \sim 1/f_{\rm l}$ is typically acceptable, and experimental results, where this is the case, are given below.

IV. Implementation and Results

This algorithm can be easily employed in most programmable PAWG systems. The first step toward compensating for distortions in the system is to acquire its transfer function $H(f)$. This can be accomplished without disrupting the system's operation. To do so, the PAWG is programmed to generate a very short optical pulse with a temporal envelope whose spectral bandwidth exceeds the bandwidth of the RF portion in the system. This pulse is then launched into the photodetector and passes through the RF amplifiers, isolators, cables, and connectors, and the output of the system is monitored on a high-speed sampling oscilloscope. The oscilloscope trace shows the impulse response of the PAWG. The fast Fourier transform (FFT) of the impulse response is then numerically computed to acquire the complex transfer function of the system.

In our system, we connected the mode-locked-laser output directly into the photodetector/amplifier cascade, bypassing the SLM and fiber dispersion. Since the 200-fs optical pulses from the laser are much shorter than the temporal response of the RF components, the optical pulses act as an impulse into the system. To compute the transfer function for the entire relevant spectrum, it is necessary to resolve electrical signals with frequencies extending to the upper limit of the high-power amplifier. Since the pulses from the mode-locked laser come at periodic intervals, we were able to use a sampling oscilloscope whose bandwidth exceeded the high-power amplifier's upper operating frequency of 26.5 GHz. The impulse response is given in Fig. 7. From this impulse response, the gain and

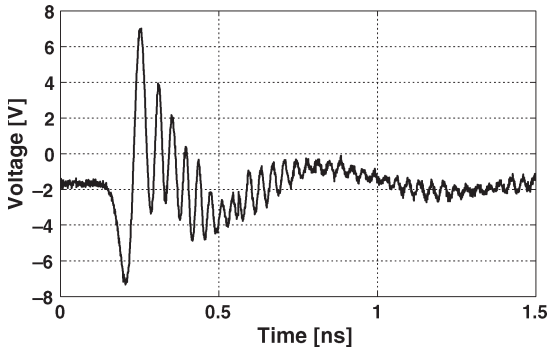

Fig. 7. Experimentally attained impulse response of the system.

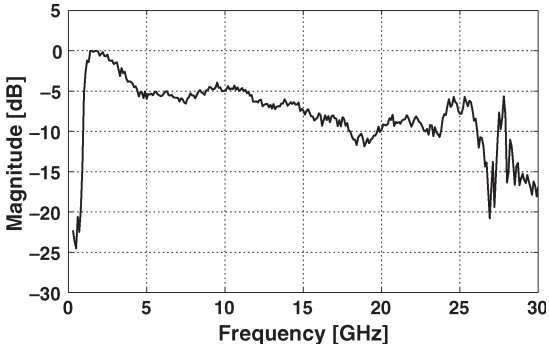

Fig. 8. Numerically computed power transfer function using the impulse-response data of Fig. 7.

phase spectra of the system were computed using the FFT. The normalized power transfer function of the system is given in Fig. 8. There is a strong resemblance to Fig. 3(a), indicating that the high-power amplifier was the dominant source of distortion in the system.

Using the transfer function derived from the impulse response, the operators $\hat{G}_1$, $\hat{G}_2$, and $\hat{G}_3$ were numerically applied onto our desired waveform to obtain the predistorted waveform $P(f)$. Note that these operators do not necessarily commute, i.e., $\hat{G}_1\hat{G}_3 \neq \hat{G}_3\hat{G}_1$. Hence, their order of application is important. In order to apply $\hat{G}_3$, it is easier to perform the raising and windowing operations in the time domain than to do the computation of (4) and (5) in the frequency domain. To do this, one first computes the inverse FFT of $\hat{G}_1 S_0$. Next, the waveform is raised so that the voltage minimum is equal to the voltage floor. The waveform is then windowed by multiplying the signal with rect(t/τ), which is nonzero during the span of the PAWG time interval. In practice, the quality of the output waveform can be enhanced by adjusting the starting point and length of this windowing interval to account for the rise and fall times of the smoother transitions in the predistorted waveform. Taking the FFT of this result yields the spectrum of the raised and windowed spectrally inverted signal. Last, the lower frequency portion of this spectrum corresponding to $f < f_{\rm L}$ is inserted into $\hat{G}_1 S_0(f)$, which is the original inverted spectrum. The inverse FFT is computed to obtain the temporal predistorted signal. A section of this signal with length τ that yields the highest fidelity output waveform is then selected.

After programming the predistorted waveform into the software of the PAWG, we observed the system's output on a

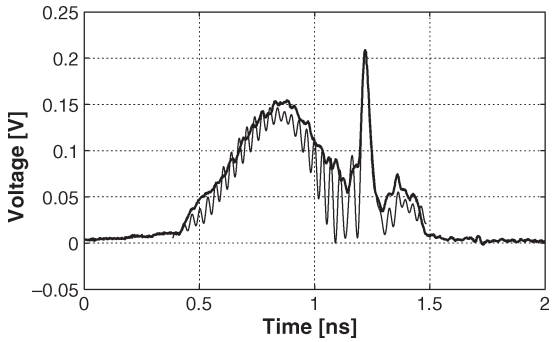

Fig. 9. Experimentally attained predistorted waveform (thick line) along with the computed ideal predistorted waveform (thin line).

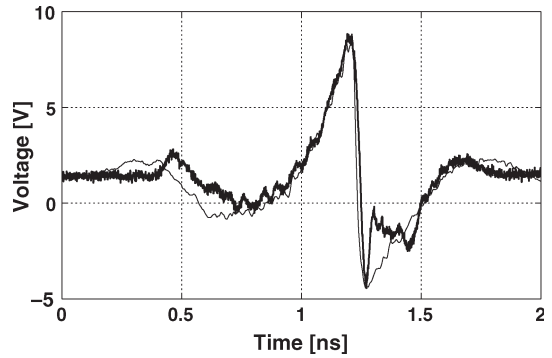

Fig. 10. Experimental results (thick line) showing the desired waveform when the predistorted waveform was input into the system. As a comparison, the theoretically best achievable waveform of Fig. 5 is also plotted (thin line).

sampling oscilloscope. Fig. 9 shows the ideal and the experimentally obtained shapes of the low power predistorted waveform. Without spectral splicing, this waveform would have to be "windowed and raised" causing sharp transitions at its edges that extended nearly half the height of this predistorted waveform. A fixed 40-dB attenuator was used to measure the high-power output waveform due to the input voltage limitations of the sampling oscilloscope. This attenuator had a flat spectral passband when measured on a vector network analyzer and, hence, had a negligible impact on the waveform fidelity.

Fig. 10 shows the output ramp produced by the high-power RF-PAWG system when the predistorted waveform is used as the input. This figure is plotted in units excluding the attenuation mentioned above, reflecting the waveform amplitude before the attenuator. The sawtooth burst shown has a rise time of 0.6 ns, a fall time of 0.1 ns, and a peak-to-peak voltage exceeding 13 V. The sinusoidal amplitude fluctuations extending the length of the burst are due to the highpass filtering by the high-power RF amplifier and are to be expected. Recall that the waveform of Fig. 5 shows the simulated result when there is no distortion in the system, except for the low-frequency attenuation by the high-power RF amplifier. The waveform of Fig. 5 is also plotted in Fig. 10 illustrating the strong overlap between the ideal case without any system distortion and the experimental result in the presence of significant distortion. It is evident that the experimental result of Fig. 10 is a dramatic improvement over the waveform of Fig. 4, which shows the output produced without using predistortion.

These experimental results demonstrate a successful RF-Photonic generation of high-speed high-power arbitrary waveforms using the spectral-splicing predistortion algorithm described in this paper. Furthermore, these results can be enhanced by additional improvements. The existing distortions in the output waveform are mainly due to the PAWG's difficulty in generating very high frequency components in the predistorted waveform (evident from Fig. 9), along with thermal and shot noise from the amplifiers. Better wavelength-to-pixel isolation and focusing of the beam before and after the 128-pixel SLM as well as using an SLM with more pixels will help yield a more accurate reproduction of the predistorted waveform. This in turn will produce a higher fidelity desired waveform. In addition, the use of a lower noise preamplifier will lessen unwanted shot noise. Further improvements to the design of a high-power broadband amplifier that decrease the lower cutoff frequency will mitigate the undesirable slow oscillations. These improvements will help to produce high-power arbitrary waveforms with even higher speeds and greater fidelity.

V. Conclusion

We have proposed and experimentally demonstrated a spectral predistortion technique designed for PAWGs, which produces complex high-power UWB waveforms in the presence of substantial RF gain and phase spectral distortions. We have implemented this technique in a burst mode RF-PAWG. Three linear operators used to create the predistorted waveform were introduced: the spectral-inversion operator, the raising operator, and the spectral-splicing operator. Together, these operators create a predistorted waveform. The spectral-inversion operator compensates for the gain and phase fluctuations of the system within its passband. In a burst mode PAWG system with significant low-frequency degradation, spectral inversion alone produces a predistorted waveform that a PAWG is unable to generate, since it has values below the voltage floor. To overcome this voltage-floor limitation, we have introduced a spectral-splicing technique that produces the necessary low frequency components and "splices" them to the signal's inverted spectrum. The application of the raising and spectral-splicing operators has produced a predistorted waveform that has smooth transitions at its edges and is physically realizable by a PAWG.

Using this algorithm, we have experimentally attained a ramped burst equivalent to one period of a sawtooth with a fundamental frequency of 1.4 GHz and a peak-to-peak amplitude greater than 13 V, corresponding to approximately 3.4 W in instantaneous power. We have generated this waveform in a system with a gain ripple of up to 5 dB and phase distortion of over 200°, which otherwise rendered a nonpredistorted waveform unrecognizable. This complex UWB waveform has a spectrum spanning more than an entire decade. Currently, it is not possible to produce such a waveform using purely electronic means. These results show the promise of photonically assisted arbitrary waveform generation for producing UWB high-power waveforms for a variety of electronic and optoelectronic applications, such as radar and optical frequency shifting.

REFERENCES

[1] S. Xiao, J. D. McKinney, and A. M. Weiner, "Photonic microwave arbitrary waveform generation using a virtually imaged phased-array (VIPA) direct space-to-time pulse shaper," *IEEE Photon. Technol. Lett.*, vol. 16, no. 8, pp. 1936–1938, Aug. 2004.

[2] M. Shen and R. A. Minasian, "Serrodyne optical frequency translation using photonics-based waveforms," *Electron. Lett.*, vol. 40, no. 24, pp. 1545–1547, Nov. 2004.

[3] T. Yilmaz, C. M. DePriest, T. Turpin, J. H. Abeles, and P. J. Delfyett, Jr., "Toward a photonic arbitrary waveform generator using a modelocked external cavity semiconductor laser," *IEEE Photon. Technol. Lett.*, vol. 14, no. 11, pp. 1608–1610, Nov. 2002.

[4] M. Hyodo, K. S. Abedin, and N. Onodera, "Generation of arbitrary optical waveforms by Fourier synthesis using three continuous-wave semiconductor lasers," *Electron. Lett.*, vol. 36, no. 3, pp. 224–225, Feb. 2000.

[5] J. Chou, Y. Han, and B. Jalali, "Adaptive RF-photonic arbitrary waveform generator," *IEEE Photon. Technol. Lett.*, vol. 15, no. 4, pp. 581–583, Apr. 2003.

[6] B. Jalali, P. Kelkar, and V. Saxena, "Photonic arbitrary waveform generator," in *Proc. LEOS 14th Annu. Meet.*, 2001, vol. 1, pp. 253–254.

[7] B. Bortnik, I. Poberezhskiy, J. Chou, B. Jalali, and H. Fetterman, "Rf-photonic generation of high-power ultrawideband arbitrary waveforms using predistortion," presented at the Optical Fiber Communication Conf. Tech. Dig., Anaheim, CA, Mar. 2006, Paper OFB6.

[8] O. Boyraz, J. Kim, M. N. Islam, F. Coppninger, and B. Jalali, "10 Gb/s multiple wavelength, coherent short pulse source based on spectral carving of supercontinuum generated in fibers," *J. Lightw. Technol.*, vol. 18, no. 12, pp. 2167–2175, Dec. 2000.

[9] J. Chou, I. Poberezhskiy, B. Bortnik, H. Fetterman, and B. Jalali, "Ultrawideband continuous sawtooth generation using RF-photonic technique," in *Proc. IEEE LTMIC*, Palisades, NY, Oct. 2004, pp. 253–254.

[10] K. K. Wong, R. M. D. L. Rue, and S. Wright, "Electro-optic-waveguide frequency translator in $LiNbO_3$ fabricated by proton exchange," *Opt. Lett.*, vol. 7, no. 11, pp. 546–548, Nov. 1982.

[11] I. Poberezhskiy, B. Bortnik, J. Chou, B. Jalali, and H. Fetterman, "Serrodyne frequency shifting of continuous optical signals using ultrawideband electrical sawtooth waveforms," *IEEE J. Quantum Electron.*, vol. 41, no. 12, pp. 1533–1539, Dec. 2005.

Bartosz Bortnik received the B.S. degree with an individual major in engineering physics and the M.S. degree in electrical engineering from the University of California, Los Angeles (UCLA), in 2001 and 2005, respectively, where he is currently working toward the Ph.D. degree.

He worked at Northrop Grumman Corporation (formerly TRW Space Technologies), Redondo Beach, CA, during the summer of 2001, where he implemented new techniques of analyzing direct digital frequency synthesizers (DDS/DDFS). He is currently with the Millimeter Wave and Optoelectronics Laboratory at UCLA, working on high-speed microwave photonic (MWP) systems.

Ilya Y. Poberezhskiy (S'01–M'04) received the B.S., M.S., and Ph.D. degrees in electrical engineering from University of California, Los Angeles (UCLA), in 1999, 2001, and 2004, respectively.

Currently, he is with the Active Optical Sensing Group at the Jet Propulsion Laboratory, California Institute of Technology, Pasadena. His research interests include optical frequency shifting, polymer electrooptic devices, and ultrafast arbitrary waveform generation. Recently, he has been working on interaction of light with large molecules and the metrology source for the upcoming Space Interferometry Mission.

Jason Chou was born in Walnut Creek, CA, on October 25, 1978. He received the B.S. (with honors) and M.S. degrees in electrical engineering from University of California, Los Angeles (UCLA), in 2000 and 2002, respectively. Currently, he is working toward a Ph.D. degree in electrical engineering at UCLA, where he conducts research in microwave photonics (MWPs) and nonlinear optics.

Bahram Jalali (S'86–M'89–SM'97–F'04) received the B.S. degree in physics from Florida State University, Talahassee, in 1989 and the M.S. and Ph.D. degrees in applied physics from Columbia University, New York, NY, in 1986 and 1989, respectively.

He is a Professor of electrical engineering, the Director of the Defense Advanced Research Projects Agency Center for Optical A/D System Technology, and the Director of the Optoelectronic Circuits and System Laboratory at the University of California at Los Angeles (UCLA). From 1988 to 1992, he was a member of the Technical Staff at the Physics Research Division, AT&T Bell Laboratories, Murray Hill, NJ, where he conducted research on ultrafast electronics and optoelectronics. While on leave from UCLA from 1999 to 2001, he founded Cognet Microsystems, a Los Angeles-based fiber-optic component company, where he served as the CEO, President, and Chairman from the company's inception through its acquisition by Intel Corporation in April 2001. From 2001 to 2004, he served as a Consultant at Intel Corporation. He has published more than 200 scientific papers. He is the holder of six U.S. patents. His current research interests are in silicon photonics and ultrafast signal processing.

Dr. Jalali is a Fellow of the Optical Society of America (OSA), the Chair of the Los Angeles Chapter of the IEEE Lasers and Electro-Optics Society (LEOS), and a member of the California NanoSystems Institute (CNSI). He was the General Chair for the IEEE International Conference on Microwave Photonics in 2001 and its Steering Committee Chair from 2001 to 2004. He serves on the Board of Trustees of the California Science Center. He was chosen by the *Scientific American Magazine* as one of the 50 Leaders Shaping the Future of Technology in 2005. He received the BridgeGate 20 Award for his contribution to the southern California economy.

Harold R. Fetterman (SM'81–F'90) received the B.A. degree in physics (with honors) from Brandeis University, Waltham, MA, in 1962 and the Ph.D. degree in physics from Cornell University, Ithaca, NY, in 1968.

He joined Lincoln Laboratory, Lexington, MA, in 1969, where his initial research concentrated on the use of submillimeter sources. In 1982, he joined the University of California, Los Angeles (UCLA), Electrical Engineering Department as a Professor and served as the first Director of the Center for High Frequency Electronics. Currently, he has programs in investigating new millimeter wave device concepts and novel means of high-frequency testing using laser techniques. He has concentrated on combining high-frequency structures and systems with optical devices.

Dr. Fetterman is a Fellow of the Optical Society of America (OSA).